SHEAR WAVE SPLITTING AT ROTOKAWA AND NGATAMARIKI GEOTHERMAL FIELDS FOR 2015

Stefan Mroczek[1], Martha Savage[1], Chet Hopp[1] and Steven Sewell[1,2]

[1]Victoria University of Wellington, PO Box 600, Wellington 6140, New Zealand

[2]Mercury, PO Box 245, Rotorua 3040, New Zealand

stefan.mroczek@vuw.ac.nz

Keywords: *Rotokawa, Ngatamariki, shear wave splitting, seismic anisotropy, fractures.*

ABSTRACT

In order to investigate the fracture orientation in the Ngatamariki and Rotokawa geothermal fields and compare them to the orientation of maximum horizontal stress, we determine the shear wave splitting for 1919 earthquakes across 22 stations during 2015.

The seismic catalogue provides a large number of microearthquakes from both fields. Due to the volume of unique events (4670), shear wave phases are picked automatically. We carry out automatic shear wave splitting measurements using the Multiple Filter Automatic Splitting Technique (MFAST). The shear wave splitting measurements are interpreted in the context of the stress in the region of Rotokawa and Ngatamariki by applying principles from circular statistics.

Preliminary results indicate that the mean fast azimuth measured from most stations in Ngatamariki agree with the expected NE-SW direction of maximum horizontal stress for the region. Stations located in Rotokawa show some tendency towards mean fast azimuths in a N-S direction, however they are generally more variable, perhaps indicating a more complex relationship between maximum horizontal stress and shear wave splitting measurements within the field.

1. INTRODUCTION

Seismic anisotropy is a material property in which a seismic wave's velocity is dependent on the direction it is travelling and on the polarisation of the wave. Shear wave splitting is a method of determining seismic anisotropy and when applied in fractured (geothermal) reservoirs it has the potential to provide a useful tool for measuring the orientation and density of fractures within the system (Elkibbi, Yang, and Rial 2005). Knowledge of the orientation and density of fractures within fields is in turn potentially useful for optimising field operations (e.g. through inclusion in numerical reservoir models) and for targeting production and injection wells.

The predominant cause of seismic anisotropy in the crust (measurable by shear wave splitting) is from fluid filled fractures which are often aligned with the maximum horizontal stress direction (Crampin and Peacock 2008). By measuring the shear wave splitting, the orientation and density of these fractures can be inferred. For an actively exploited geothermal field knowledge of these parameters could help to inform operations. Temporal variations could also indicate changes in the fractures and stress state within the reservoirs caused by field operations (e.g. increased fracturing due to stimulation around injection wells).

The geothermal fields of both Ngatamariki and Rotokawa have extensive seismic monitoring. They are also the subject of other geological and geophysical studies thus allowing comparison with other measures of stress and structure. Both fields are located within the Taupo Volcanic Zone (TVZ). The two fields' proximity to each other allows earthquakes from both fields to be studied together.

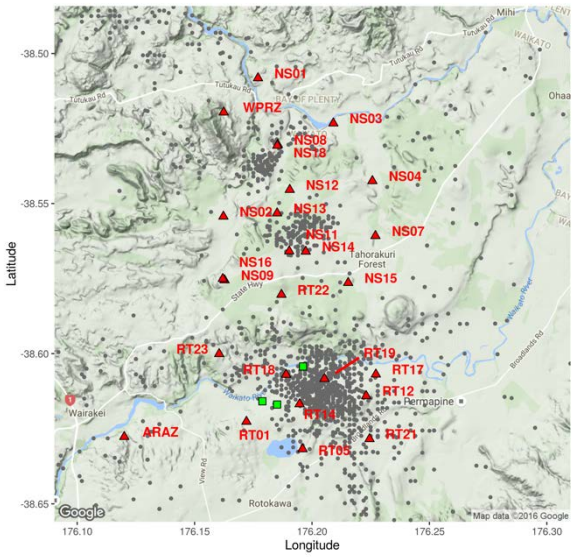

Figure 1: Events with at least one high grade shear wave splitting measurement for 2015 with station locations marked in red. Northern clusters are located in Ngatamariki while the southern cluster is located in Rotokawa. Green squares show wellhead locations for wells studied by Massiot et al. (2015) and McNamara, Massiot, et al. (2015).

Micro-earthquake events used for this shear wave splitting analysis are those from the 2015 catalogue from the region encompassing both fields, enhanced with 2466 additional detections using the matched-filter technique, made by Hopp et al. (this volume). The detections included are those which are detected on at least nine stations and which have a correlation of greater than 0.5 with their template. Automatic S-wave picking, using spickerC of Castellazzi et al. (2015) (Section 2.1), allows approximately 23% of events detected on a single station to have their shear wave phase determined. Due to the volume of events picked we have been able to employ statistical methods and tests including clustering and comparison of means, all of which require a sufficiently large numbers of measurements. In total 1919 unique events were used (Figure 1).

Sherburn et al. (2013) consider most of the seismicity at Rotokawa to be induced by deep reinjection of condensate and brine. It is likely that the seismicity at Ngatamariki is induced by similar mechanisms whereby the pre-fractured

rock is contracted by cool reinjected fluids allowing fractures to reactivate (Sherburn et al. 2013).

1.1 Shear wave splitting

Shear wave splitting occurs when a shear wave enters an anisotropic medium and is split because the component polarised in one particular direction travels faster than the orthogonal component (Savage 1999). Shear wave splitting is characterised by two variables: fast azimuth (polarisation), φ, controlled by the anisotropic symmetry system and its orientation, and delay time, δt, between the arrival of the fast and orthogonal polarisations (Savage 1999). The fast azimuth is an axial quantity so has a 180° ambiguity (a fast azimuth of 0° is the same as one of 180°). In many statistical operations an axial quantity can be conveniently treated as a simple direction by doubling the angle value, performing the operation and then halving the result.

The prevalent cause of shear wave splitting in the upper crust is likely to be fluid filled fractures that align with the local orientation of maximum horizontal stress (S_{Hmax}) (Crampin and Peacock 2008). Fast azimuths are controlled by both the anisotropic medium and the propagation direction, but for many systems the fast directions are similar for a wide range of propagation angles (e.g. Babuska and Cara (1991)). Fractures not aligned with S_{Hmax} tend to be closed and their fluid forced into vertical fractures aligned with S_{Hmax}. Thus the fast azimuth aligns with the local direction of S_{Hmax} and the delay time gives an indication of the fracture density along the station-event path.

Various studies have observed that, when close to faults, measured fast azimuths align with the fault strike (e.g. Evans et al. (1995), Zhang and Schwartz (1994), Zinke and Zoback (2000)). This alignment may be due to fractures or rock fabric resulting from fault parallel shear (Evans et al. 1995). The TVZ is a normal faulting regime so S_{Hmax} is expected to be parallel to the strike of the faults. Shear wave splitting resulting from either fractures or faults may be indistinguishable from each other in special cases when the faults align with S_{Hmax} (e.g. in a normal faulting regime).

Measures of S_{Hmax} regionally from focal mechanisms (Townend et al. 2012) and more locally from borehole features from three boreholes in Rotokawa (McNamara, Massiot, et al. 2015) provide a comparison for fast azimuth measurements. Fracture distributions from cores and televiewer logs in Rotokawa (Massiot et al. 2015) also provide direct information on the orientation and density of fractures that may be causing the anisotropy being measured. The large-scale geological structure of the Rotokawa and Ngatamariki reservoirs is also well known (McNamara, Sewell, et al. 2016, Chambefort et al. 2016).

In this paper we report measurements of shear wave splitting in Ngatamariki and Rotokawa and use cluster analysis of station-event paths to interpret the results in terms of fracture and stress orientation.

2. METHODS

2.1 Automatic S-picking

Shear wave splitting measurements require the shear wave phase to be determined. The volume of events in the catalogue make manual picking time prohibitive so instead an automatic phase picker is used, spickerC of Castellazzi et al. (2015).

spickerC uses a combination of three different detection and picking methods: short term average versus long term average ratio (STA/LTA) as described by Allen (1978), polarisation detection based on the approach of Cichowicz (1993) and autoregressive picking using the Akaike Information Criterion (AR-AIC) as described by Leonard and Kennett (1999). The final pick is a weighted mean of the three methods with a final grade based on the error estimate and the signal to noise ratio around the pick (Castellazzi et al. 2015).

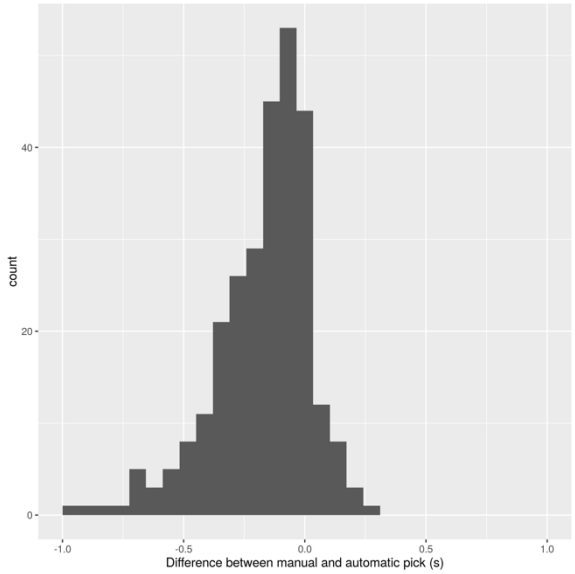

Figure 2: Time difference between earliest AR-AIC pick and manual pick for all stations in Rotokawa during 2013.

The automatic shear wave picking program (S-picker) was originally written by Diehl et al. (2009). The version used here was modified from version 1.4.0 for use with local earthquakes in New Zealand by Castellazzi et al. (2015). S-picker was used by Castellazzi et al. (2015) in conjunction with MFAST (shear wave splitting program) to make automatic picking and splitting measurements at Ruapehu Volcano in New Zealand. Corrections and modifications were made to S-picker (updating to version 1.4.0.a) by Castellazzi et al. (2015) and are described therein. This most recent version of S-picker (1.4.0.a), used in processing here, is known as spickerC.

spickerC categorises its automatic picks into classes depending on their assigned error value. The class0 category is the category with the lowest error. In this study class0 picks have an error of ≤ 0.3 seconds and a signal to noise ratio (SNR) of ≥ 3. Picks in the class0 category are those which are then processed in MFAST. Following the method of Castellazzi et al. (2015), we use the earliest AR-AIC pick from the class0 category. This better approximates manual picks as well as being what is expected by MFAST (Castellazzi et al. 2015).

2.1.1 spickerC parameters

spickerC was trained using one hundred manually picked events detected in 2013 from station RT01, located in Rotokawa (Greenbank 2014). The parameters used in spickerC were chosen in a trial and error process. Initial values were set similarly to those of Castellazzi et al. (2015) with some modifications based on the change in setting from volcanic to geothermal. The parameters were then varied individually. After a parameter was changed spickerC was rerun. An increase in the number of class0 picks was considered a positive change and was kept, while no change

or a decrease in class0 picks was reverted. Those parameters which changed from Castellazzi et al. (2015) are shown in Table 1.

Most changes to parameters resulted in a change of less than 10 in the number of class0 picks. Increasing the band of allowable Vp/Vs (P-wave to S-wave velocity ratio), from that of Castellazzi et al. (2015), almost doubled the number of class0 picks made from 40 to 74.

Before picking, data was filtered with both a high pass (0.5 Hz) and a Wood-Anderson filter. The Wood-Anderson filter integrates to displacement and acts like a low pass filter (Nabelek, Braunmiller, and Phillips 2013). The Vp/Vs band was set to between 1.2 and 2.0 (mean of 1.6).

Figure 2 shows the difference between the earliest AR-AIC automatic pick and the manual pick from events in Rotokawa from March to June 2013 (Greenbank 2014) with eight outliers greater than one second removed. Most picks lie within half a second of each other however the distribution is skewed to the left with a mean of -0.17 seconds (manual picks are generally made at later times than the earliest corresponding AR-AIC pick). This is likely due to manual picks not always selecting the earliest arrival of the split shear wave.

Table 1: spickerC parameters changed from Castellazzi et al. (2015) (Ruapehu data). See the Supporting information of Castellazzi et al. (2015) for parameters and their descriptions.

Parameter	Old Val.	New Val.
sta (sec)	0.2	0.15
lta (sec)	2	1.5
tup (sec)	0.2	0.1
tdw (sec)	0.1	0.05
Noise model window (sec)	1.2	1.1
Signal model window (sec)	1.2	1.1
Order noise model	10	15
Order signal model	10	16

2.2 Automatic shear wave splitting (MFAST)

Shear wave splitting measurements are made using the Multiple Filter Automatic Splitting Technique (MFAST) of Savage et al. (2010a), Wessel (2010). Here we briefly summarise the method contained therein.

MFAST uses a combination of the Silver and Chan (1991) splitting method (with corrections from Walsh, Arnold, and Savage (2013)) and cluster analysis of splitting measurements (Teanby, Kendall, and Van der Baan 2004). The waveforms are bandpass filtered and the three best filters are selected based on the product of signal to noise ratio and the bandwidth of the filter. The splitting measurements are made on each of these best filters. Measurements are made by running the splitting algorithm on a set of windows each with different splitting parameters. The best windows are those whose parameters best remove the splitting. The best window is selected using the cluster analysis of Teanby, Kendall, and Van der Baan (2004). The measurements are graded based on the standard deviations of the clusters and how consistent the clusters are with each other (Savage et al. 2010a).

Measurements are graded null if fast azimuth is within 20 degrees of the incoming S polarisation. In this study, measurements with delay time less than 80% of the maximum time delay (0.2 seconds), signal to noise ratio greater than three, error in fast azimuth of less than 20 degrees and with an A or B cluster grade were kept for further analysis and are henceforth referred to as high grade measurements. If events have high grade measurements from more than one of their three best filters the one from the best filter is chosen.

MFAST requires an S pick (for a located earthquake) which in this case we made using spickerC (see previous section).

2.2.1 MFAST parameters

The most common bandpass filter selected in processing was 1 - 30 Hz. Mean delay time for the (high grade) data is 0.087 seconds. The main MFAST parameters are listed in Table 2. Refer to the MFAST manual (Wessel, Savage, and Teanby 2016) for a description of these parameters. The “very local” variation of the MFAST codes is used in processing.

Table 2: MFAST processing parameters. See Wessel, Savage, and Teanby (2016).

Parameter	Value
t_win_snr	3 s
t_err	0.05 s
SNRmax	3
tlagmax	0.2 s
dtlagmax	0.05 s
twin_freq	3 s

2.3 Earthquake path clustering

Clustering events by their location is useful as it provides an indication of where measured anisotropy originates. When investigating temporal changes it also allows migration of the seismicity to be ruled out as a cause of changing anisotropy.

Seismicity is generally confined to a single area in Rotokawa and two distinct areas in Ngatamariki. Clustering these events purely by location proved inadequate for three reasons. Firstly, to be able to recover statistically significant means the clusters had to contain a sufficient number of measurements. Secondly, doing a simple clustering with k-means gave clusters which contained all events from a particular field, thus the assumption that events in a cluster have a similar location no longer holds. Finally, given that shear wave splitting is measured not at a point but rather along the station-event path, it is more intuitive to cluster the station-event paths so that events with similar paths to the same station group together.

To approximate this clustering we calculate the pierce points of the station-event paths on a unit sphere below each station (Figure 3). A pierce point is the location where a path intersects a surface. Only stations with more than 55 measurements are clustered using this method as sufficiently large samples are required. Mixtures of von Mises-Fisher distributions (the spherical equivalent of a normal distribution) are then fit to the pierce points using the movMF package (Hornik and Grün 2014) in the R software environment (R Core Team 2013). This clusters the pierce points by location on the sphere (each distribution is fit to a set of pierce points which form a cluster).

Data for each station is clustered separately. The clustering (movMF) algorithm (Hornik and Grün 2014) requires that the number of clusters be set before running. The clustering is repeated with one to seven clusters being fit to the pierce points. The best number of clusters is chosen using the Bayesian Information Criterion. This is a comparative measure of how well a model fits the observations with a penalty for adding more clusters to prevent over fitting. The number of clusters which minimises the criterion for a particular station is chosen and the corresponding clustering is kept.

To determine if the fast azimuths of events within a specific cluster depart from circular uniformity (i.e. there is a dominant fast azimuth) the Rayleigh test is used. The Rayleigh test is a statistical test for circular uniformity. If the concentration of data points around a circle is above a certain threshold then the hypothesis that there is circular uniformity (no dominant mean direction) is rejected (Pewsey, Neuhäuser, and Ruxton 2013). This test is carried out on the (doubled) fast azimuths from the events in each of the clusters determined by movMF. If the p-value from the Rayleigh test is less than 0.1 the test is considered a pass and the cluster is determined to have a statistically significant mean fast azimuth. The p-value indicates the significance of the mean direction where 0.1 indicates that there is a small amount of evidence for a single mean fast azimuth while a p-value of 0.01 indicates strong evidence for a single mean fast azimuth.

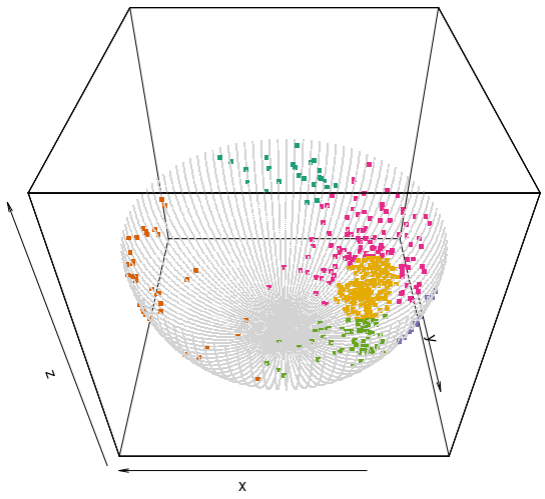

Figure 3: Pierce points on sphere beneath station RT01. Colours represent different path clusters. The yellow cluster gives a statistically significant fast azimuth originating from events in Rotokawa.

For stations with more than one cluster of paths which pass the Rayleigh test the mean fast azimuths of these clusters were compared using the bootstrap version of Watson's Nonparametric test following the method of Fisher (1993) (Pewsey, Neuhäuser, and Ruxton 2013). If there is less than medium evidence (p-value >0.05) that the means from each cluster are different they are grouped together. The test is non-parametric so allows us to test for equality of means without needing to specify the distributions of the data within the clusters. Bootstrapping allows clusters with smaller sample sizes to be included.

Clusters with a wide range of station-event paths generally fail the Rayleigh test, suggesting such measurements from clusters should be inspected on an event by event basis and that spatial variation in anisotropy is present.

At angles of incidence greater than 35° (where vertical incidence is 0°) converted phases can interfere with shear wave splitting measurements at the surface (Nuttli 1961, Booth and Crampin 1985). Measurements with angles of incidence below 35° fall into the shear wave window where measurements are free of this interference. Figure 3 is calculated using straight line paths (i.e. uniform velocity model) and, due to low velocity layers near the surface, many studies consider events below 45° to be in the shear wave window (e.g. Volti and Crampin 2003). However, this is too restrictive and so removes too many useful events (Savage et al. 2010b). This is especially true in geothermal areas which are characterised by low velocities. For example, 64% of events with angles of incidence greater than 45° on Figure 3 are in fact within the shear wave window when angles of incidence are calculated using a more accurate velocity model. If we restrict the measurements to include only those within 35° incidence using the Rotokawa velocity model of Rawlinson (2011), the average fast directions are significantly different from the full dataset at only one station (RT05) using Watson's nonparametric test (described earlier in this section). Thus, for this study, we choose not to remove measurements based on their angle of incidence.

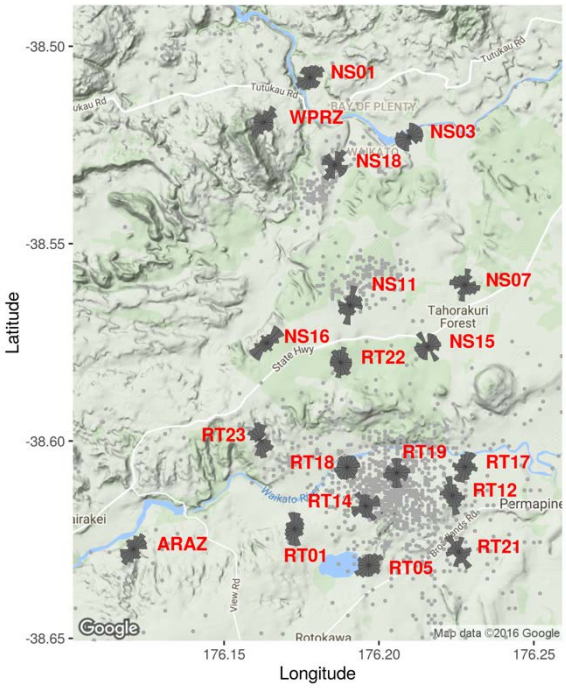

Figure 4: Fast azimuth rose plots.

3. RESULTS

3.1 Station Results

The Rayleigh test (described in Section 2.3) is used to divide the stations into two categories: those with a single dominant fast azimuth for all measurements (which pass the Rayleigh test with a p-value less than 0.05) and those with uniformly distributed fast azimuths (which fail). These are described in Section 3.1.1 and 3.1.2 respectively.

Rose plots of fast azimuths measured at each station are shown in Figure 4. Stations NS04 and NS02 are excluded, both having less than three measurements. NS12-NS14 are borehole stations and do not have their orientation calibrated, so all measurements of fast azimuth will have an unknown

fixed offset. They are also not reported here. During the study period two stations were disbanded and moved slightly. To account for this we merge the measurements post processing. NS09 and NS16 are merged (labelled NS16) and NS08 and NS18 are merged (labelled NS18). There is no significant evidence that the mean fast azimuth of each station differs after being moved (using Watson's Nonparametric test as described in Section 2.3).

Across all stations, 23% of events (for each station) were successfully picked using spickerC. 34% of these picked events gave high grade shear wave splitting measurements. Thus, roughly 8% of catalogue events (for an individual station) result in high grade shear wave splitting measurement. The rate of successful S-wave picks is lower than the 28% of Castellazzi et al. (2015) which is due to the addition of matched-filter detections to our catalogue (there 27% successful pick rate when excluding matched filter detections). The rate of high grade shear wave splitting measurements from our picks is significantly lower, 34% versus 60% of of Castellazzi et al. (2015) (Ruapehu data), perhaps in part due to difference in the maximum delay time used in MFAST processing. Our study area being much smaller, we only consider events with a time delay of below 0.16 seconds to be high grade, versus 0.6 seconds in Castellazzi et al. (2015). Also, Castellazzi et al. (2015) only includes events of magnitude 1.5 and above while in this study we have no minimum magnitude.

Table 3: Stations with a dominant fast azimuth. Columns are: mean fast azimuth (degrees from north), standard error, number of events, number of events with s-wave picked and number of high grade shear wave splitting measurements.

Station	F.A.(°)	S.E.(°)	Events	Picks	Me.
ARAZ	34	8.7	1771	266	39
WPRZ	43	3.3	3752	534	346
NS01	37	7.0	2963	999	253
NS03	57	4.6	1700	288	474
NS11	31	11	1636	165	46
NS16	49	2.6	2285	480	148
RT01	9	2.4	3824	1415	489
RT05	51	5.0	3233	1835	555
RT12	-19	3.8	2742	909	253
RT17	26	5.6	3021	742	250
RT23	-19	7.2	1141	126	33

3.1.1 Dominant fast azimuth

The mean fast azimuth for Ngatamariki (NS & WPRZ stations) along with ARAZ fall into the band of 31° to 57° (Table 3). The mean orientation of S_{Hmax} in the TVZ, measured from focal mechanisms (Townend et al. 2012), is NE-SW (39.38° to 50.62° by standard definition) or ENE-WSW (61.88° to 73.12°). The mean fast azimuth of all these stations are within one standard error of these S_{Hmax} orientations. In situ-borehole measurements of S_{Hmax} orientation made in Rotokawa by McNamara, Massiot, et al. (2015) also agree with the observed fast azimuths for these stations.

Stations in Rotokawa (RT) have mean fast azimuths distributed around a N-S orientation ranging from -19° to 26° with RT05 as an outlier with an mean of 51°.

Standard errors, quoted for each station in Table 3, provide a measure of how close the sample mean is to the mean of the underlying population of fast azimuths. Here we calculate the standard error by re-sampling (with replacement) the doubled fast azimuths and calculating the mean of the re-sampled values. Re-sampling is where values are drawn randomly from a sample, in this case the sample is the fast azimuths from a single station. This is repeated 9999 times with the mean calculated each time. The standard error is the standard deviation of these means. The standard error is halved to give the standard error of the axial mean fast azimuths (see Section 1.1).

Table 4: Stations with uniformly distributed fast azimuths. Columns are: number of events, number of events with s-wave picked and number of high grade shear wave splitting measurements.

Station	Events	Picks	Measurements
NS07	1547	131	39
NS15	1119	185	52
NS18	1364	163	49
RT14	2879	355	73
RT18	3258	1067	274
RT19	3209	259	26
RT21	2783	123	36
RT22	524	119	29

Table 5: Earthquake path clusters. Columns are: mean fast azimuth (degrees from north), standard error and number of events with splitting measurement.

Station	F.A.(°)	S.E.(°)	Measurements
WPRZ	41	3.0	222
NS01	44	13.7	50
NS03	65	4.5	61
NS16	41	12.2	74
RT01 (N)	11	4.3	113
RT01 (S)	25	9.5	63
RT01 (Fig6)	5	2.5	238
RT05 (Fig5)	-6	8.7	46
RT05 (Fig6)	44	9.1	190
RT12	-17	3.2	193
RT17	31	6.3	114

3.1.2 Uniformly distributed fast azimuths

Mean fast azimuths are not quoted for stations which fail the Rayleigh test as they are not statistically significant. Table 4 shows a summary of these stations. Ngatamariki stations (NS) without a dominant fast azimuth generally all have a small number of measurements. It is likely that, with additional measurements, a dominant azimuth would become apparent.

Rotokawa stations (RT) with a large number of measurements and uniformly distributed fast azimuths are generally located much closer to seismicity than other stations which pass the test (see Figure 1).

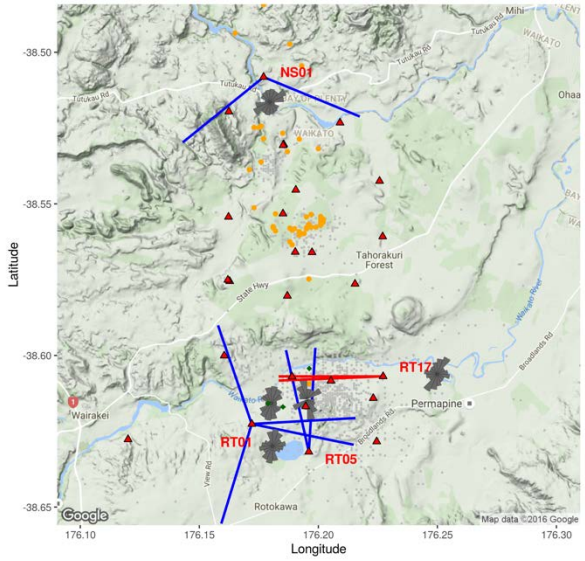

Figure 5: Fast azimuth rose plots from station-event path clusters outside of red cones and within blue cones. Events making up RT05's N-S cluster are highlighted in orange.

3.2 Path clustering

Figure 5 and 6 show the result of the path clustering method in Section 2.3. Means are summarised in Table 5. All measurements for each rose diagram have station-event paths which lie within the cones formed by blue lines or outside for those with red lines. This gives an indication of where the measured anisotropy is originating.

Stations RT01, RT12 and RT17 all show that their N-S character originates from the main Rotokawa cluster. RT17 and RT12 only have very narrow bands of paths which have been excluded. RT01 also has two smaller path clusters which originate outside of the main Rotokawa cluster which also have N-S mean fast azimuths.

Station RT05 has one cluster with a strong N-S component (-6°) typical of Rotokawa stations (orange in Figure 5). However, the earthquakes making up this cluster originate largely from southern Ngatamariki rather than from the main body of Rotokawa events.

Most of the anisotropy observed in Ngatamariki originates along the path from Rotokawa.

4. DISCUSSION

Station RT18 has a large number of high grade shear wave splitting measurements associated with it yet fails the Rayleigh test and thus do not appear to have any dominant fast azimuth. Stations RT14 and RT19 also fail although these two stations do have a smaller number of measurements. All three of these stations are located much closer to the main group of Rotokawa earthquakes, which produce their splitting measurements, than stations with dominant azimuths. Stations located slightly further away (e.g RT01, RT12, RT17) tend to pass the Rayleigh test and have a roughly N-S orientation. Ngatamariki stations with a larger number of events (>60) all pass the Rayleigh test and all have mean fast azimuths closer to the expected NE-SW trend of stress in the region. RT05 appears to be in-between these two extremes where it passes the Rayleigh test but has a low concentration around its mean fast azimuth. Without the addition of matched-filter detections to the catalogue RT05 fails the Rayleigh test while still having a large amount of measurements (282).

It is possible that whatever is causing stations close to seismicity to have uniformly distributed fast azimuths is also related to the anomalous N-S trend. However, one of the clusters from RT05 has a strong N-S character while the events in the cluster are located in Ngatamariki (highlighted in orange on Figure 6). This suggests that the N-S character is local to Rotokawa and not a side effect of the observed uniformly distributed fast azimuths. Along with NE-SW and ENE-WSW S_{Hmax} orientations, McNamara, Massiot, et al. (2015) also measured NNE-SSW which match with RT17. N-S orientated cracks are also common in all three boreholes. Massiot et al. (2015) also identified a family of fractures in Rotokawa boreholes with N-S orientations perhaps indicating a relationship with the N-S fast azimuths observed in Rotokawa. Wellhead locations are plotted in green on Figure 1 (RK32, RK30L1 and RK18L2).

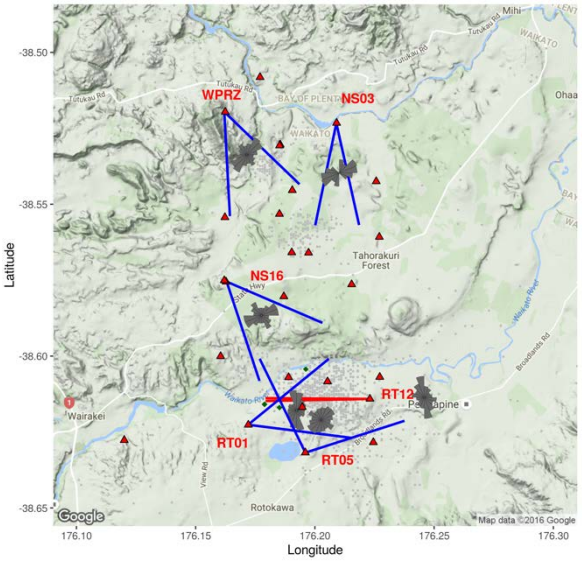

Figure 6: Fast azimuth rose plots from station-event path clusters outside of red cones and within blue cones.

5. CONCLUSIONS

The orientation of mean fast azimuths determined in the study for Rotokawa and Ngatamariki is 28° to 57° with rotation to a broader range of orientations centred N-S within the Rotokawa field.

Of stations with a dominant fast azimuth, those in Ngatamariki and station ARAZ (all located outside of Rotokawa) have mean fast azimuths which coincide with the expected values of NE-SW to ENE-WSW from in-situ and regional measurements (McNamara, Massiot, et al. 2015, Townend et al. 2012). The mean fast azimuths of stations located in Rotokawa fell into a broader range of -21° to 38° centred on an N-S orientation.

Clustering of station-event paths revealed that the NE-SW character of stations outside Rotokawa largely originated from events within Rotokawa. While Rotokawa stations measured N-S anisotropy from the seismicity within the field,

station RT05 showed some events originating in Ngatamariki which also have a N-S orientation. This suggests that the N-S mean fast azimuths measured in Rotokawa are local to the field and not a result of proximity to the seismicity. N-S fractures are common in all three boreholes located in Rotokawa measured by McNamara, Massiot, et al. (2015).

6. FUTURE WORK

Further investigation into why stations located close to seismicity may be failing the Rayleigh test is required.

Preliminary tests indicate no statistically significant change in time for most path clusters. The addition of more years to the catalogue will allow temporal changes to be investigated. This would also allow the measurements to be broken into time periods expected to show differences (e.g. after significant stimulation). Also, stations which failed the Rayleigh test tended to only have a small number of measurements so an increase in events would be beneficial.

Three borehole stations (NS12 to NS14) are not orientated. Work to correctly orientate these stations will add a significant amount of high quality measurements in the centre of the Ngatamariki field as well as providing a comparison between borehole and surface stations.

The Rayleigh test only tests the significance of a single mean fast azimuth. Thus stations which potentially have more than one mean fast azimuth (i.e sampling more than one population of anisotropy) could fail. Investigation into stations which potentially have more than one mean fast azimuth could give more information about the origin of anisotropy in Rotokawa.

In addition, shear wave splitting tomography, similar to that of Johnson, Savage, and Townend (2011) could be used to identify regions of differing anisotropy and to investigate temporal changes.

ACKNOWLEDGEMENTS

We would like to thank Mercury and the Rotokawa Joint Venture (Mercury and Tauhara No.2 Trust) for their support of this research in awarding an MSc scholarship to Stefan Mroczek, providing access to data and permission to publish this work. We are also grateful to GeoNet for providing the earthquake data.

Figures were made using the ggplot2 (Wickham 2009) and ggmap (Kahle and Wickham 2013) packages. Statistical analysis was carried out using the circular package of Agostinelli and Lund (2013). All packages are within the R software environment (R Core Team 2013). The Seismic Analysis Code was used in the processing of seismic data (Helffrich, Wookey, and Bastow 2013).

REFERENCES

Agostinelli, C. and Lund, U.: R package circular: Circular Statistics (version 0.4-7). CA: Department of Environmental Sciences, Informatics and Statistics, Ca' Foscari University, Venice, Italy. UL: Department of Statistics, California Polytechnic State University, San Luis Obispo, California, USA, 2013.

Allen, R.V.: Automatic earthquake recognition and timing from single traces. *Bulletin of the Seismological Society of America* 68.5 (1978).

Babuska, V. and Cara, M.*: Seismic anisotropy in the Earth.* Vol. 10. Springer Science & Business Media, 1991.

Booth, D.C. and Crampin, S.: Shear-wave polarizations on a curved wavefront at an isotropic free surface. *Geophysical Journal International* 83.1 (1985).

Castellazzi, C., et al.: Shear wave automatic picking and splitting measurements at Ruapehu volcano, New Zealand. *Journal of Geophysical Research. Solid Earth* 120.5 (2015).

Chambefort, I., et al.: Ngatamariki Geothermal Field, New Zealand: Geology, geophysics, chemistry and conceptual model. *Geothermics* 59 (2016).

Cichowicz, A.: An automatic S-phase picker. *Bulletin of the Seismological Society of America* 83.1 (1993).

Crampin, S. and Peacock, S.: A review of the current understanding of seismic shear-wave splitting in the Earth's crust and common fallacies in interpretation. *Wave Motion* 45.6 (2008).

Diehl, T., et al.: Automatic S-wave picker for local earthquake tomography. *Bulletin of the Seismological Society of America* 99.3 (2009).

Elkibbi, M., Yang, M. and Rial, J.A.: Crack-induced anisotropy models in The Geysers geothermal field. *Geophysical Journal International* 162.3 (2005).

Evans, J.R., et al.: Shear-wave splitting from local earthquakes at The Geysers geothermal field, California. *Geophysical Research Letters* 22.4 (1995).

Fisher, N.I.: Statistical analysis of circular data. (1993).

Greenbank, E. Seismic anisotropy and fractures at Rotokawa Geothermal Field. Unpublished manuscript.

Helffrich, G., Wookey, J. and Bastow, I.: *The Seismic Analysis Code: A Primer and User's Guide.* Cambridge University Press, 2013.

Hopp, C., et al.: Matched filter earthquake detection and double difference relocation at Rotokawa and Ngatamariki geothermal areas: January to November, 2015. This volume.

Hornik, K. and Grün, B.: movMF: An R Package for Fitting Mixtures of von Mises-Fisher Distributions. *Journal of Statistical Software* 58.10 (2014).

Johnson, J.H., Savage, M.K. and Townend, J.: Distinguishing between stress-induced and structural anisotropy at Mount Ruapehu Volcano, New Zealand. *Journal of Geophysical Research: Solid* Earth 116.B12 (2011).

Kahle, D. and Wickham, H.: ggmap: Spatial Visualization with ggplot2. *The R Journal* 5.1 (2013).

Leonard, M. and Kennett, B.L.N.: Multi-component autoregressive techniques for the analysis of seismograms. *Physics of the Earth and Planetary Interiors* 113.1 (1999).

Massiot, C., et al.: Fracture Width and Spacing Distributions from Borehole Televiewer Logs and Cores in the Rotokawa Geothermal Field, New Zealand. *Proceedings World Geothermal Congress 2015*. (2015)

McNamara, D.D., Massiot, C., et al.: Heterogeneity of structure and stress in the Rotokawa Geothermal Field, New Zealand. *Journal of Geophysical Research: Solid Earth* 120.2 (2015).

McNamara, D.D., Sewell, S., et al.: A review of the Rotokawa Geothermal Field, New Zealand. *Geothermics* 59 (2016).

Nabelek, J.L., Braunmiller, J. and Phillips, W.S.: Source and path calibration in regions of poor crustal propagation using temporary, large-aperture, high-resolution seismic arrays. Tech. rep. 2013.

Nuttli, O.: The effect of the Earth's surface on the S wave particle motion. *Bulletin of the Seismological Society of America* 51.2 (1961).

Rawlinson, Z.: Microseismicity associated with actively exploited geothermal systems: earthquake detection and probabilistic location at Rotokawa and statistical seismic network design at Kawerau. MSc thesis. Victoria University of Wellington, 2011.

R Core Team. R: A Language and Environment for Statistical Computing. Vienna, Austria: R Foundation for Statistical Computing, 2013.

Savage, M.K.: Seismic anisotropy and mantle deformation: What have we learned from shear wave splitting? *Reviews of Geophysics* 37.1 (1999).

Savage, M.K., et al.: Automatic measurement of shear wave splitting and applications to time varying anisotropy at Mount Ruapehu volcano, New Zealand. *Journal of Geophysical Research, Solid Earth* 115.12 (2010a).

Savage, M.K., et al.: Stress magnitude and its temporal variation at Mt. Asama Volcano, Japan, from seismic anisotropy and GPS. *Earth and Planetary Science Letters* 290.3 (2010b).

Sherburn, S., et al.: Microseismicity at Rotokawa geothermal field, 2008 to 2012. Proceedings of the 35th New Zealand geothermal workshop. Rotorua, New Zealand. (2013).

Silver, P.G. and Chan, W.W.: Shear wave splitting and subcontinental mantle deformation. *Journal of Geophysical Research: Solid Earth* 96.B10 (1991).

Teanby, N.A., Kendall, J.M. and Van der Baan, M.: Automation of shear-wave splitting measurements using cluster analysis. *Bulletin of the Seismological Society of America* 94.2 (2004).

Townend, J., et al.: Three-dimensional variations in present-day tectonic stress along the Australia–Pacific plate boundary in New Zealand. *Earth and Planetary Science Letters* 353 (2012).

Volti, T. and Crampin, S.: A four-year study of shear-wave splitting in Iceland: 1. Background and preliminary analysis. *Geological Society, London, Special Publications* 212.1 (2003).

Walsh, E., Arnold, R. and Savage, M.K.: Silver and Chan revisited. *Journal of Geophysical Research. Solid Earth* 118.10 (2013).

Wessel, A.: Shear Wave Splitting Measurements at Mt. Ruapehu Volcano, New Zealand. MSc thesis. Victoria University of Wellington, 2010.

Wessel, A., Savage, M.K. and Teanby, N.A.: Manual for the Multiple Filter Automatic Splitting Technique (MFAST) processing codes, Version 2.1. Victoria University of Wellington, 2016.

Wickham, H.: *ggplot2: Elegant Graphics for Data Analysis*. Springer-Verlag New York, 2009.

Zhang, Z. and Schwartz, S.Y.: Seismic anisotropy in the shallow crust of the Loma Prieta segment of the San Andreas fault system. *Journal of Geophysical Research: Solid Earth* 99.B5 (1994).

Zinke, J.C. and Zoback, M.D.: Structure-related and stress-induced shear-wave velocity anisotropy: observations from microearthquakes near the Calaveras Fault in Central California. *Bulletin of the Seismological Society of America* 90.5 (2000).